Evaluation of phosphate ion adsorption from aqueous solution by nickel-aluminum complex hydroxides

Fumihiko Ogata, Megumu Toda, Masashi Otani, Takehiro Nakamura and Naohito Kawasaki

ABSTRACT

We prepared a variety of nickel-aluminum complex hydroxides, investigated their physicochemical properties, and evaluated their ability to adsorb phosphate ions (the molar ratios of nickel to aluminum, 1:2, 1:1, 2:1, 3:1, and 4:1, are referred to as NA12, NA11, NA21, NA31, and NA41). NA12 and NA11 have amorphous structures; their specific surface areas and the concentration of associated hydroxyl groups were greater than those of other adsorbents. The number of phosphate ions adsorbed onto NA12 and NA11 was greater than that onto other adsorbents. These results indicated that the phosphate ion adsorption is related to the specific surface area and the amount of hydroxyl groups. The adsorption isotherm data, and the effects of contact time and pH on the adsorption were investigated; our results implied that both the Freundlich equation model and the pseudo-second-order kinetic model describe the adsorption of phosphate ions by NA11. We showed that phosphate ions adsorbed onto NA11 can be desorbed by sodium hydroxide solution at different concentrations and that NA11 could be reused for at least three repeated cycles of phosphate ion adsorption and desorption. This study illustrates that NA11 has the potential for practical application as an adsorbent for phosphate ions from wastewater.

Key words | adsorption, nickel-aluminum complex hydroxide, phosphate ion

Fumihiko Ogata
Takehiro Nakamura
Naohito Kawasaki (corresponding author)
Faculty of Pharmacy,
Kindai University,
3-4-1 Kowakae, Higashi-Osaka, Osaka 577-8502,
Japan
E-mail: *kawasaki@phar.kindai.ac.jp*

Megumu Toda
Masashi Otani
Kansai Catalyst Co., Ltd,
1-3-13, Kashiwagi-cho, Sakai-ku, Sakai, Osaka 590-0837,
Japan

Naohito Kawasaki
Antiaging Center,
Kindai University,
3-4-1 Kowakae, Higashi-Osaka, Osaka 577-8502,
Japan

INTRODUCTION

Phosphates, as essential and often limiting nutrients in most aquatic environments, can result in the acceleration of eutrophication, which leads to an increase in costs associated with water treatment and poses a potential threat to human health and the ecological balance (Dodds *et al.* 2008). At the same time, phosphorus resources in the world may only last 50 to 100 years. Therefore, for both these reasons, it is necessary to effectively remove (or adsorb) phosphate ions from aqueous solutions (Laroussi *et al.* 2003; Choe *et al.* 2004; Bennett & Elser 2011).

Currently, numerous methods such as chemical precipitation, electrocoagulation, crystallization, adsorption, reverse osmosis, and biological treatments are available for the removal of phosphate ions from wastewater (Den & Shi 2015). Among these methods, the adsorption process shows advantages of being operationally straightforward, highly efficient, and relatively inexpensive. Various types of adsorbents have been tested for phosphate ion adsorption (Yang *et al.* 2014). In recent years, the development of composite adsorbents containing two or more different metal oxides for phosphate ion adsorption has gained increasing attention (Li *et al.* 2014). Previous studies have reported on the use of Fe-Co binary oxide, Zn-Al LDH, Zr-Fe oxide nanoparticles, Fe-Mn binary oxide, and Fe-Mn-Al trimetal oxide for the adsorption of phosphate ions from aqueous solution. Composite adsorbents exhibit superior adsorption performance, since they possess the inherent advantages of their parent materials (Zhang *et al.* 2009; Lü *et al.* 2013; Li *et al.* 2014; Yu *et al.* 2015; Zhang *et al.* 2017).

In our previous studies, which focused on enhancing phosphate ion adsorption, we found that nickel-cobalt binary hydroxide showed excellent adsorption of phosphate ions from aqueous solution (Ogata *et al.* 2017). However, cobalt is expensive and has the potential to adversely affect health and the aquatic environment (including the biota). Consequently, we investigated materials to replace cobalt in the adsorbent and reported that aluminum oxides have excellent potential to adsorb phosphate ions

doi: 10.2166/wst.2018.273

(Kawasaki *et al.* 2008). In the aforementioned study, we anticipated that nickel-aluminum complex hydroxides would be promising as adsorbents for phosphate ions. However, until now, no systematic investigation of phosphate ion adsorption by nickel-aluminum complex hydroxides has been reported.

Therefore, the object of this study was to explore the feasibility of using composite metal oxides derived from nickel and aluminum for the adsorption of phosphate ions. An investigation of the physicochemical characteristics of nickel-aluminum complex hydroxides was conducted. Their kinetic and isothermal behavior was investigated, and the parameters influencing phosphate ion adsorption, including solution pH and adsorption temperatures, were also studied. Additionally, desorption of phosphate ions from nickel-aluminum hydroxides was performed to assess their regeneration capacity.

MATERIAL AND METHODS

Materials

Nickel-aluminum complex hydroxides with molar ratios of Ni^{2+} to Al^{3+} of 4.0, 3.0, 2.0, 1.0, and 0.5, referred to as NA41, NA31, NA21, NA11, and NA12, respectively, were prepared by the co-precipitation method. The characteristics of the adsorbents were investigated: the specific surface area, morphologies, and crystallinities were measured using a NOVA 4200*e* specific surface analyzer (Yuasa Ionic, Japan), scanning electron microscopy (SEM, SU1510, Hitachi High-Technologies Co., Japan), and X-ray diffractometry (XRD, MiniFlex II, Rigaku, Japan), respectively. The number of hydroxyl groups was measured using the fluoride ion adsorption method reported by Yamashita *et al.* (1978). The surface pH of the adsorbent was measured using a digital pH meter F-73 (HORIBA, Ltd, Japan). Briefly, the adsorbent (0.1 g) was added to distilled water of pH 7.0 (50 mL), the suspensions were shaken for 2 min at 25 °C, and filtered through a 0.45 μm membrane filter. Elemental analysis and electron spectroscopy were carried out using an electron microanalyzer (EPMA, JXA-8530F, JEOL, Japan) and an X-ray photoelectron spectroscopy system (AXIS-NOVA, Shimadzu Co., Ltd, Japan), respectively.

The sample solution of phosphate ions was prepared by potassium dihydrogen phosphate. The solution pH was adjusted by hydrochloric acid and sodium hydroxide solution. All reagents (special reagent grade) were purchased from Wako Pure Chemical Industries, Ltd, Japan.

Adsorption of phosphate ions

The adsorbent (0.05 g) was added to 50 mL of a 300 mg/L phosphate ion solution. The suspension was shaken at 100 rpm for 24 h at 25 °C. Subsequently, the sample was filtered through a 0.45 μm membrane filter, and then the filtrate was analyzed using adsorption spectrophotometry (DR/890, HACH, USA). The equilibrium concentration of phosphate ions was determined using the ascorbic acid reduction method (Kofinas & Kioussis 2003). The amount of phosphate ions adsorbed was calculated using Equation (1):

$$q = (C_0 - C_e)/VW \quad (1)$$

where q is the amount of phosphate ions adsorbed (mg/g), C_0 is the initial concentration and C_e is the equilibrium concentration of phosphate ions (mg/L), V is the solvent volume (L), and W is the weight of the adsorbent (g).

In addition, the concentration of sulfate ions in the filtrate was measured by ion chromatography (DIONEX ICS-900, Thermo Fisher Scientific Inc., Japan). The measurements were performed using the IonPac AS12A system (4 × 200 mm, Thermo Fisher Scientific Inc., Japan). The mobile phase and the regenerant comprised 2.7 mmol/L Na_2CO_3 + 0.3 mmol/L $NaHCO_3$ and 12.5 mmol/L H_2SO_4, respectively. The flow rate was 1.0 mL/min at ambient temperature. The micro membrane suppressor was an AMMS 300 system (4 mm, Thermo Fisher Scientific Inc., Japan) and the sample volume was 10 μL.

Effect of solution pH, contact time, and temperature on the adsorption of phosphate ions

First, a number of samples were prepared by adding 0.05 g of adsorbent (NA11) to 50 mL of a 50 mg/L phosphate ion solution. The suspension pH was adjusted by hydrochloric acid or sodium hydroxide solution to obtain a range of 2.0–12.0, and then the sample solutions were shaken at 100 rpm for 24 h at 25 °C. Secondly, the adsorbent (NA11, 0.05 g) was added to a 50 mL of a 50 mg/L phosphate ion solution. The suspensions were shaken for 1, 3, 5, 8, 12, 16, 20, and 24 h at 100 rpm at 25 °C. Finally, the adsorbent (NA11, 0.05 g) was added to 50 mL of phosphate ion solution that had concentrations ranging from 10 to 100 mg/L. The suspensions were shaken for 24 h at 100 rpm at 5, 25, and 45 °C. The amount of phosphate ion adsorbed in each case was calculated using Equation (1).

Adsorption and desorption capability for phosphate ions

In this case, the adsorbent (NA11, 0.3 g) was added to 100 mL of a 300 mg/L phosphate ion solution. The suspensions were shaken for 24 h at 100 rpm at 25 °C. Subsequently, the sample was filtered through a 0.45 μm membrane filter, then the filtrate was analyzed using adsorption spectrophotometry (DR/890, HACH, USA). The amount of phosphate ions adsorbed was calculated using Equation (1). After adsorption treatment, the NA11 was collected, dried, and then used for the desorption treatment. The collected NA11 was added to 100 mL volumes of sodium hydroxide solution having concentrations of 1, 10, 100, and 1,000 mmol/L. Then, the suspensions were shaken for 24 h at 100 rpm at 25 °C, after which, they were filtered through a 0.45 μm membrane filter. The concentration of phosphate ions released from the NA11 was measured using an adsorption spectrophotometer. The amount desorbed was calculated using Equation (2).

$$d = C_e V / W \tag{2}$$

where d is the amount of phosphate ions desorbed (mg/g), C_e is the concentration after the desorption (mg/L), V is the solvent volume (L), and W is the weight of the adsorbent sample (g). Additionally, the potential for repeated use of the NA11 in subsequent recoveries of phosphate ions was evaluated by repeating the abovementioned treatment (adsorption and desorption treatment is one cycle) three times. Sodium hydroxide solution at a concentration of 1,000 mmol/L was used in this experiment.

RESULTS AND DISCUSSION

Properties of the adsorbents

Figure 1 shows SEM images of the adsorbents. A hexagonal crystal system was observed in NA41 and NA31, but an irregular crystal system was noted with increasing amounts of aluminum. These phenomena indicated that the constituent elements (aluminum and nickel) affect the crystal system. Additionally, the changes of crystal system were slightly between NA12 and NA41. The XRD patterns of the adsorbents (shown in Figure 2) were consistent with powder diffraction file 2010 obtained from the International Center for Diffraction Data, indicating that all the adsorbents consisted mainly of nickel hydroxide. In addition, NA41 had a highly crystalline nature, which decreased with increasing amounts of aluminum, suggesting that NA12 and NA11 (amorphous nature) are highly reactive. Table 1 shows the characteristics of the adsorbents. Specific surface areas and the concentration of hydroxyl groups in NA were greater with increasing amounts of aluminum. NA12 (specific surface area: 26.4 m^2/g, concentration of hydroxyl groups: 1.62 mmol/g) and NA11 (specific surface area: 22.8 m^2/g, concentration of hydroxyl groups: 1.92 mmol/g) have high specific surface areas and hydroxyl group concentrations. However, the constituent element ratios did not appear to significantly affect the surface pH in this study (pH 6.50–7.98).

Amount of phosphate ions adsorbed using NAs

The amount of saturated phosphate ions adsorbed is shown in Figure 3; NA41 adsorbed the least (70.2 mg/g), and

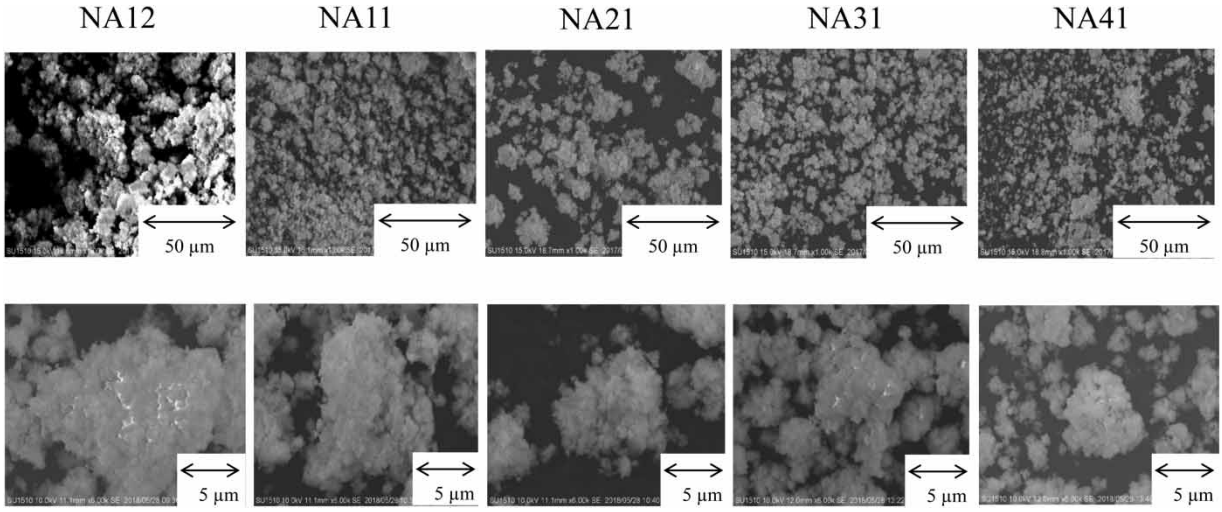

Figure 1 | SEM images of adsorbents.

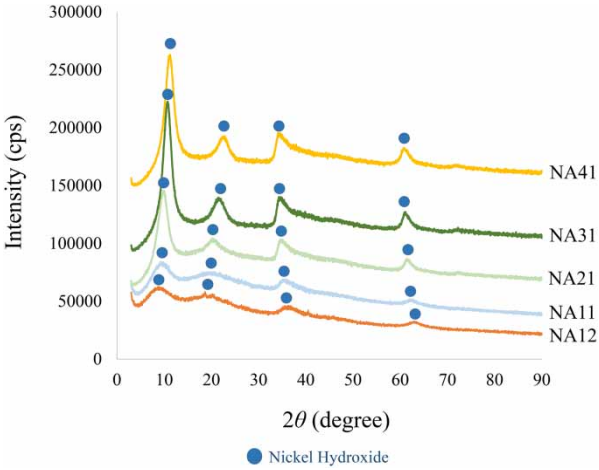

Figure 2 | XRD patterns of the adsorbents.

Table 1 | Properties of the adsorbents

Samples	Specific surface area (m^2/g)	Amount of hydroxyl groups (mmol/g)	Surface pH
NA41	14.6	0.80	7.28
NA31	11.7	0.82	6.50
NA21	15.6	1.05	7.04
NA11	22.8	1.92	7.98
NA12	26.4	1.62	7.63

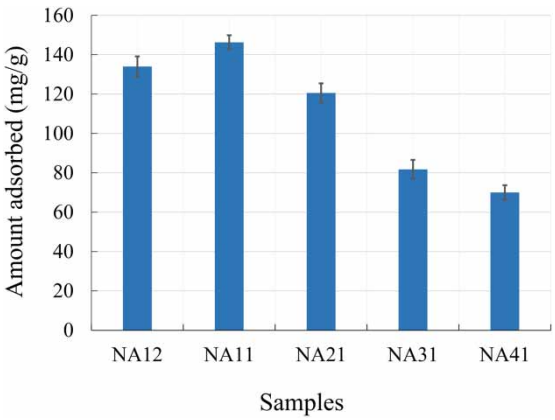

Figure 3 | The amount of saturated phosphate ions adsorbed. Initial concentration: 300 mg/L, solution volume: 50 mL, temperature: 25 °C, amount adsorbent: 0.05 g, agitation speed: 100 rpm, contact time: 24 h.

adsorption increased in the order NA31 (82.1 mg/g) < NA21 (121.1 mg/g) < NA12 (134.9 mg/g) < NA11 (146.8 mg/g). The adsorption capacity of NA11 was also greater than those reported previously for other adsorbents (Kawasaki *et al.* 2008, 2010; Ogata *et al.* 2016, 2017). These results indicate that the nickel-aluminum complex hydroxide is an efficient adsorbent of phosphate ions from aqueous solutions.

In addition, we evaluated the relationship between the amount adsorbed and the characteristics of the adsorbent to elucidate the adsorption mechanism of phosphate ions. First, the relationship between the specific surface area or the number of hydroxyl groups and the amount of phosphate ions adsorbed was evaluated. The correlation coefficients were 0.818 and 0.918, respectively, which indicated that the amounts adsorbed are related to the specific surface area and the number of hydroxyl groups. Second, we observed the adsorbent surface before and after adsorption (Figure 4) and recorded an increase in phosphorus content after the adsorption treatment. We interpret this observation to mean that one of the adsorption mechanisms of phosphate ions using NA may involve a combination of electrostatic interaction, ligand exchange, and ion exchange (Yang *et al.* 2014). Third, we measured the binding energy of the adsorbent surface (NA11) before and after the adsorption treatment (Figure 5). After adsorption, P(2s) and P(2p) peaks were detected and the S(2p) peak intensity was significantly reduced, which suggested that phosphate ions combined with NA11 and, at the same time, sulfate ions were released (the NA was prepared using sulfates). Finally, we measured the concentration of phosphate and sulfate ions after adsorption (data not shown). We confirmed that the amounts of phosphate ions adsorbed by NA11 and the amounts of sulfate ions released were positively correlated in this experiment (correlation coefficient: 0.837), supporting the theory that sulfate ions interlayered in the NA are exchanged with phosphate ions in the sample solutions. The aforementioned mechanisms are similar to those reported by previous studies (Li *et al.* 2014; Lu *et al.* 2014; Yang *et al.* 2014; Yu *et al.* 2015; Wang *et al.* 2018). However, the release of sulfate ion is not good point in the wastewater treatment. Therefore, if NA11 is applied in the field, it must be considered the sulfate ion concentration after adsorption treatment. In addition, Table 2 shows the comparison of phosphate ion adsorption capacity of NA11 with other reported adsorbents. It is evident that the phosphate ion adsorption capacity of NA11 is higher than that of other adsorbents. Therefore, this result indicated that NA11 has the greatest potential for the adsorption of phosphate ion from the aqueous phase.

Effect of solution pH on the adsorption of phosphate ions

The effect of solution pH on the adsorption of phosphate ions is shown in Figure 6; the amount adsorbed at an initial

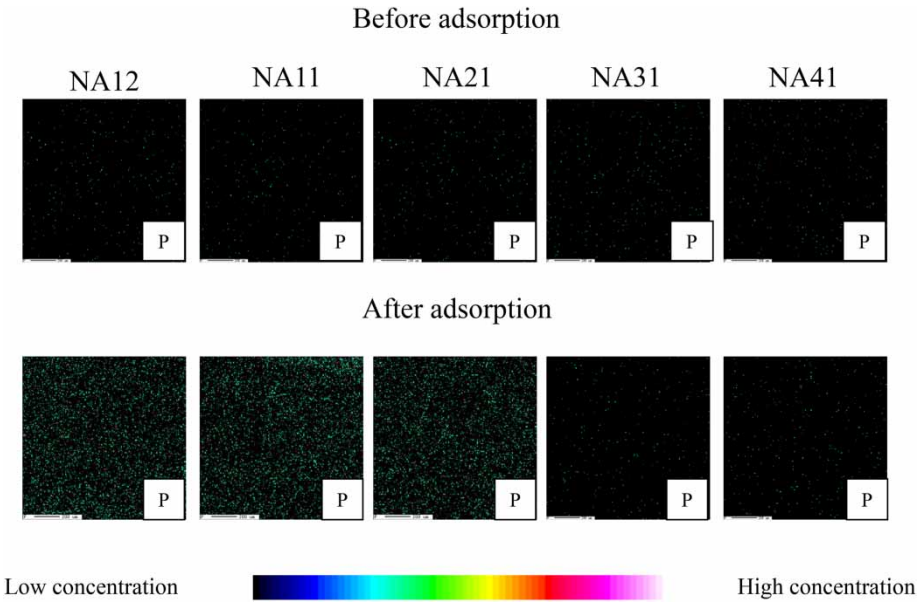

Figure 4 | Qualitative analysis of the adsorbent surface before and after adsorption of phosphate.

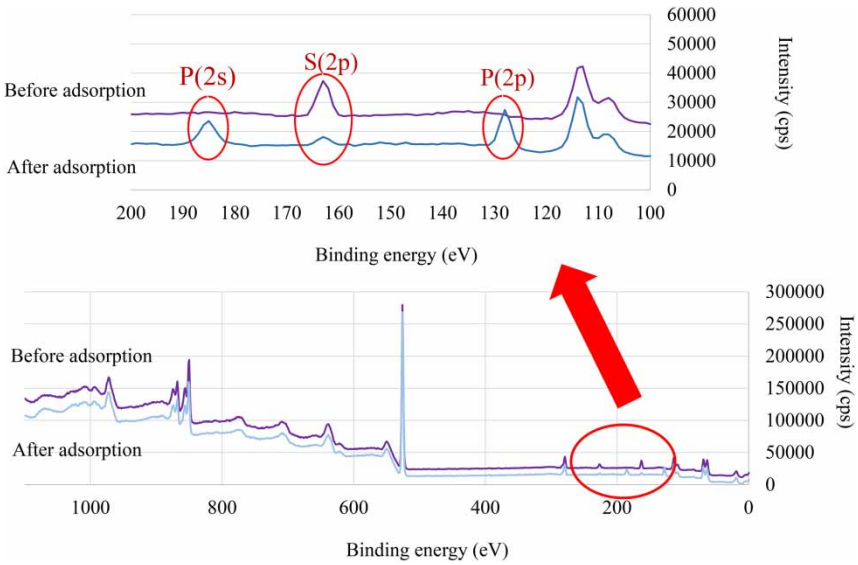

Figure 5 | Binding energy of phosphorus and sulfur before and after adsorption onto NA11.

pH of 4.0 to 10.0 (equilibrium pH is 6.2–7.7) was greater than that at an initial pH of 2.0 (equilibrium pH is 3.2). When the pH value is between 3.0 and 7.2, the main species in solution is monovalent $H_2PO_4^-$, while at a pH between 7.2 and 11.0, the predominant species of phosphate is HPO_4^{2-} (Rodrigues & de Silva 2009). Previous studies indicated that the $H_2PO_4^-$ species were more easily adsorbed on the metal (hydr)oxide surface than other species (Rodrigues & de Silva 2009; Lai *et al.* 2016). In addition, the results demonstrated that NA11 has a buffering capacity. This phenomenon could also explain why no obvious changes in the amount of adsorbed phosphate ions were observed in the pH range between 4.0 and 10.0. Consequently, it seems likely that NA11 would be suitable for the adsorption of phosphate ions from environmental water for a realistic range of operational conditions.

Table 2 | Comparison of phosphate ion adsorption capacity of NA11 with other reported adsorbents

Adsorbents	Adsorption capacity (mg/g)	Reference
Mg-Al hydrotalcite-loaded kaolin clay	11.9	Den & Shi (2015)
Modified iron oxide-based sorbents	38.8	Lalley *et al.* (2016)
Fe-Cu binary oxide	39.8	Li *et al.* (2014)
Composite metal oxide	26.3	Liu *et al.* (2012)
Zirconium(IV) loaded cross-linked chitosan particles	71.7	Liu *et al.* (2016)
Mg-Al LDH	31.3	Yang *et al.* (2014)
Zn-Al LDH	68.4	Yang *et al.* (2014)
Pyromellitic acid intercalated ZnAl-LDHs	57.1	Yu *et al.* (2015)
Magnetic zirconium-iron oxide nanoparticle	21.3	Zhang *et al.* (2017)
NA11	146.8	This study

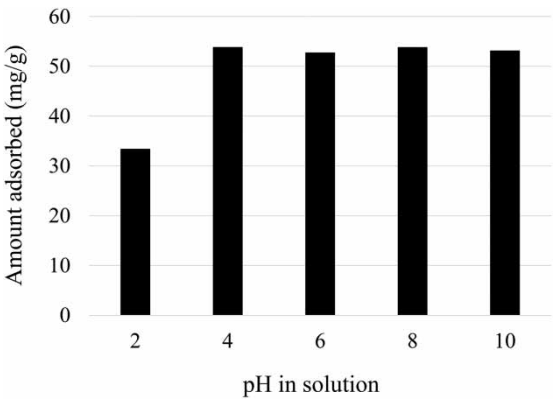

Figure 6 | Amount of phosphate ions adsorbed onto NA11 at different pH condition. Initial concentration: 50 mg/L, solution volume: 50 mL, temperature: 25 °C, amount adsorbent: 0.05 g, agitation speed: 100 rpm, contact time: 24 h, pH: 2–12.

Effect of contact time on the adsorption of phosphate ions

Batch experiments were conducted to explore the rate of phosphate ion adsorption onto NA11. The initial adsorption of phosphate ions onto NA11 was rapid within 3 h (46.4 mg/g) but slowed down as equilibrium (49.8 mg/g) was approached (equilibrium adsorption time was less than 6 h). Pseudo-first-order (Equation (3)) and pseudo-second-order (Equation (4)) kinetic models were used to represent the kinetics of phosphate ion adsorption. The kinetic models can be expressed as

$$\ln(q_e - q_t) = \ln q_e - k_f t \tag{3}$$

$$\frac{t}{q_t} = \frac{1}{k_s q_e^2} + \frac{t}{q_e} \tag{4}$$

where q_e and q_t are the amounts (mg/g) of phosphate ions adsorbed at equilibrium and at time t (h), respectively; k_f is the rate constant of the pseudo-first-order model adsorption (1/h); and k_s is the rate constant of the pseudo-second-order model adsorption (g/mg/h).

The kinetic data of the adsorption of phosphate ions onto NA11 were fitted to the pseudo-first-order kinetic model and pseudo-second-order kinetic model; the calculated parameters are listed in Table 3. From comparisons of the correlation coefficients (r), it is evident that the fit of the pseudo-second-order model (1.000) is better than pseudo-first-order model (0.969), although it can be seen from the correlation coefficients that both models fit the data well. In addition, the amount of adsorbent calculated, $q_{e,cal}$ (50.3 mg/g), in the pseudo-second-order model was closer to the actual experimental amount of adsorbent used, $q_{e,exp}$ (49.8 mg/g). These results indicate that chemisorption is possibly the dominant mechanism in this adsorption reaction (Sposite 1984; Lu *et al.* 2014).

Table 3 | Kinetic parameters for the adsorption of phosphate ions

		Pseudo-first-order model			Pseudo-second-order model		
Sample	$q_{e,exp}$ (mg/g)	k_f (1/h)	$q_{e,cal}$ (mg/g)	r	k_s (g/mg·h)	$q_{e,cal}$ (mg/g)	r
NA11	49.8	0.22	7.8	0.969	1.7×10^{-6}	50.3	1.000

Adsorption isotherms of phosphate ions onto NA11

The amount of phosphate ions adsorbed by NA11 increases with increasing temperature; the temperature dependence of the adsorption capacity of different aqueous equilibrium concentrations can be illustrated by adsorption isotherms (Figure 7). The Langmuir and Freundlich isotherm models were used to investigate the equilibrium adsorption data. The Langmuir isotherm model assumes that the adsorbent is structurally homogeneous; namely, the adsorption process results in a monolayer with uniform adsorption energies, and there is no interaction among the adsorbed molecules. On the other hand, the Freundlich isotherm model can be applied to multilayer adsorption on surfaces with heterogeneous energetic distribution of active sites; in contrast to the Langmuir model, there is interaction among the adsorbed molecules (Liu *et al.* 2016).

The Langmuir isotherm equation is given as:

$$\frac{C_e}{q_e} = \frac{1}{W_s a} + \frac{C_e}{W_s} \tag{5}$$

where C_e is the equilibrium concentration (mg/L); q_e is the amount adsorbed at equilibrium (mg/g); and W_s and a are Langmuir constants relating to the monolayer adsorption capacity and energy of sorption, respectively. The Freundlich adsorption equation, for a particular temperature, is as follows:

$$\log q_e = \log k + \left(\frac{1}{n}\right) \log C_e \tag{6}$$

where q_e is the adsorption capacity (mg/g) of the adsorbate, C_e is the equilibrium concentration (mg/L) of the adsorbate,

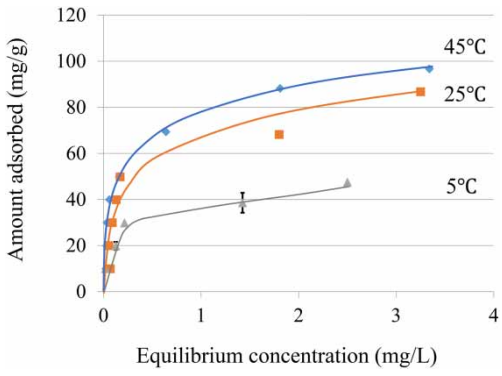

Figure 7 | Adsorption isotherms of phosphate ions onto NA11 at different temperatures. Initial concentration: 10–100 mg/L, solution volume: 50 mL, temperature: 5, 25, and 45 °C, amount adsorbent: 0.05 g, agitation speed: 100 rpm, contact time: 24 h.

Table 4 | Freundlich and Langmuir constants for the adsorption of phosphate ions

		Freundlich constants			Langmuir constants		
Sample		**1/n**	**logk**	**r**	**Ws (mg/g)**	**a (L/mg)**	**r**
NA11	5 °C	0.29	1.56	0.987	47.9	13.1	0.960
	25 °C	0.34	1.75	0.857	113.6	2.6	0.764
	45 °C	0.36	1.88	0.899	142.9	4.4	0.878

and k and n are the Freundlich constants related to the adsorption of the adsorbent and the intensity of adsorption, respectively.

Table 4 shows the Freundlich and Langmuir constants for the adsorption of phosphate ions; the correlation coefficients of the respective isotherm models are 0.857–0.987 and 0.764–0.960. The Langmuir constant (W_s) increased with increasing adsorption temperatures (5–45 °C), which corresponded to the trend observed in the data in Figure 7. In addition, phosphate ions were easily adsorbed onto the surface of NA11 when $1/n$ was in the range 0.1–0.5, but not when $1/n > 2$ (Abe *et al.* 1967). The data obtained in our research ($1/n$: 0.29–0.36) suggested that the adsorption of phosphate ions on the NA11 surface occurred readily, as a result of chemisorption. In the present study, NA11 was produced by the co-precipitation method, which might lead to a more heterogeneous surface of NA11; therefore, the Freundlich equation would be more suitable to describe the isotherm data (Lu *et al.* 2014).

Adsorption thermodynamics

In order to evaluate the adsorption process and determine its thermodynamic properties, thermodynamic parameters, including the changes in enthalpy (ΔH) and entropy (ΔS), and the Gibbs free energy (ΔG) of the adsorption, were determined from experimental data using the equations that follow (Den & Shi 2015; Wang *et al.* 2018):

$$\Delta G = -\mathrm{RT}\ln K \tag{7}$$

$$\ln K = \frac{-\Delta H}{RT} + \frac{\Delta S}{R} \tag{8}$$

where R (8.134 J/mol K) is the gas constant, T (K) is the absolute temperature, and K is the standard thermodynamic equilibrium constant defined as q_e/C_e. In the plot of ln K versus $1/T$, ΔH and ΔS can be estimated from the slopes and intercept, respectively.

The thermodynamic parameters for the adsorption of phosphate ions onto NA11 are shown in Table 5. The positive

Table 5 | Thermodynamic parameters for the adsorption of phosphate ions

Sample	ΔH (kJ/mol)	ΔS (J/(mol K))	ΔG (kJ/mol) at temperature		
			278 K	298 K	318 K
NA11	2.23	23.4	−4.31	−4.65	−5.26

value of ΔH (2.23 kJ/mol) confirmed the endothermic nature of the adsorption and was in good agreement with the experimental results reported elsewhere (Yu *et al.* 2015). In addition, the ΔG value decreased from − 4.31 to −5.26 kJ/mol when the temperature was increased from 278 to 318 K, implying an increase in the spontaneity of the reactions (Liu *et al.* 2012). In addition, the ΔG values were greater than −20 kJ/mol, suggesting that electrostatic interaction played a significant role in the adsorption process (Weng *et al.* 2007). The positive ΔS value (23.4 J/mol K) implied that the randomness increased at the solution/solid interface during the adsorption process (Zhang *et al.* 2017).

Adsorption/desorption capacity of NA11 for phosphate ions

To determine the reusability of the used NA11, its regeneration (using sodium hydroxide at different concentrations) and re-adsorption were investigated. It could be seen that the amounts of phosphate ions desorbed increased with increasing alkalinity. The phosphate ion desorption percentages were 0.5% (amount adsorbed and amount desorbed is 93 mg/g and 0.4 mg/g, respectively), 9.4% (amount adsorbed and amount desorbed is 93 mg/g and 8.7 mg/g, respectively), 25.3% (amount adsorbed and amount desorbed is 93 mg/g and 23.5 mg/g, respectively), and 74.2% (amount adsorbed and amount desorbed is 93 mg/g and 69.0 mg/g, respectively) for 1, 10, 100, and 1,000 mmol/L sodium hydroxide solutions, respectively. These results suggested that the bonds between the active sites and the adsorbed phosphate ions are breakable, and the phosphate ions adsorbed into NA11 can be exchanged by hydroxide under high-pH conditions; thus, NA11 has the potential to be used as a renewable adsorbent (Maor *et al.* 2011). These adsorption–desorption cycles using 1,000 mmol/L sodium hydroxide solution were carried out up to three times; the results are presented in Figure 8. The adsorption percentages of phosphate ions slowly decreased with an increase in the number of regeneration cycles (the total amount adsorbed, total amount desorbed, and total recovery percentage are 225 mg/g, 197 mg/g, and 88%, respectively). The adsorption loss might be due to the extraction of effective constitute (nickel and aluminum) in NA11 and the incomplete

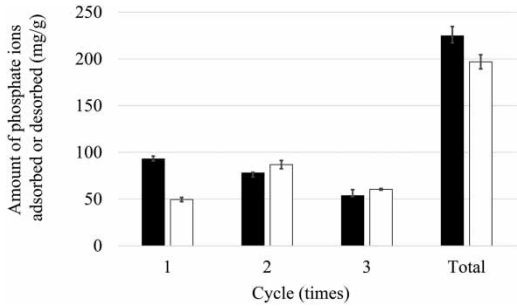

Figure 8 | Amount of phosphate ions adsorbed or desorbed using NA11. Adsorption condition; initial concentration: 300 mg/L, sample volume: 100 mL, adsorbent: 0.3 g, temperature: 25 °C, contact time: 24 h, 100 rpm, desorption condition; sample volume: 100 mL, temperature: 25 °C, contact time: 24 h, 100 rpm, ■: amount adsorbed, □: amount desorbed.

phosphate ion desorption using alkaline solution as an eluent, especially for inner phosphate ion complexes. Nevertheless, the regenerated NA11 was still cost-effective for phosphate ion adsorption and could be reused at least three times. Thus, the adsorption of phosphate ions onto NA11 is relatively reversible and it appears that NA11 can be regenerated via sodium hydroxide solution treatment (Maor *et al.* 2011; Liu *et al.* 2012; Li *et al.* 2014).

CONCLUSIONS

Adsorbents (nickel-aluminum complex hydroxides, NA12, 11, 21, 31, and 41) were prepared in order to investigate their phosphate ion adsorption capacity. NA11 had an amorphous structure with a large specific surface area (22.8 m^2/g) and a high concentration of hydroxyl groups (1.92 mmol/g). We elucidated that the adsorption mechanism of phosphate ions was related to the above-mentioned properties. In addition, we measured the elemental composition and the binding energy before and after adsorption, which supported the hypothesis that adsorbent surfaces are an important factor for the adsorption of phosphate ions. Ion exchange with the sulfate ions in NA11 was also involved in the adsorption of phosphate ions ($r = 0.837$). The amount of phosphate ions adsorbed increased with increasing temperature, and these data were fitted to the Freundlich equation model ($r = 0.857$–0.987). In addition, thermodynamic and kinetic experiments demonstrated that the phosphate ion adsorption was a spontaneous, endothermic chemisorption. The phosphate-loaded NA11 could be effectively regenerated by sodium hydroxide solution and reused at least three times for phosphate ion adsorption. Thus, NA11 appears to be a promising candidate for the adsorption of phosphate ions from aqueous solution.

ACKNOWLEDGEMENTS

MEXT (Ministry of Education, Culture, Sports, Science and Technology)-supported Program for the Strategic Research Foundation at Private Universities, 2014–2018 (S1411037).

REFERENCES

Abe, I., Hayashi, M. & Kitagawa, M. 1976 Studies on the adsorption of surfactants on activated carbon. *Journal of Japan Oil Chemists' Society* **25**, 145–150.

Bennett, E. & Elser, J. 2011 A broken biogeochemical cycle. *Nature* **478**, 29–31.

Choe, S., Liljestrand, H. M. & Khim, J. 2004 Nitrate reduction by zero-valent iron under different pH regimes. *Applied Geochemistry* **19**, 335–342.

Den, L. & Shi, Z. 2015 Synthesis and characterization of a novel Mg-Al hydrotalcite-loaded kaoline clay and its adsorption properties for phosphate in aqueous solution. *Journal of Alloys and Compounds* **637**, 188–196.

Dodds, W. K., Bouska, W. W., Eitzmann, J. L., Pilger, T. J., Pitts, K. L., Riley, A. J., Schioesser, J. T. & Thornbrugh, D. J. 2008 Eutrophication of U.S. freshwaters: analysis of potential ecomonic damages. *Environmental Science & Technology* **43**, 12–19.

Kawasaki, N., Ogata, F., Takahashi, K., Kabayama, M., Kakehi, K. & Tanada, S. 2008 Relationship between anion adsorption and physicochemical properties of aluminum oxide. *Journal of Health Science* **54**, 324–329.

Kawasaki, N., Ogata, F. & Tominaga, H. 2010 Selective adsorption behavior of phosphate onto aluminum hydroxide gel. *Journal of Hazardous Materials* **181**, 574–579.

Kofinas, P. & Kioussis, D. R. 2003 Reactive phosphorus removal from aquaculture and poultry productions systems using polymeric hydrogels. *Environmental Science & Technology* **37**, 423–427.

Lai, L., Xie, Q., Chi, L., Gu, W. & Wu, D. 2016 Adsorption of phosphate from water by easily separable Fe_3O_4@SiO_2 core/shell magnetic nanoparticles functionalized with hydrous lanthanum oxide. *Journal of Colloids and Interface Science* **465**, 76–82.

Lalley, J., Han, C., Li, X., Dionysiou, D. D. & Nadagouda, M. N. 2016 Phosphate adsorption using modified iron oxide-based sorbents in lake water: kinetics, equilibrium and column test. *Clinical Engineering Journal* **284**, 1386–1396.

Laroussi, M., Mendis, D. A. & Rosenberg, M. 2003 Plasma interaction with microbes. *New Journal of Physics* **5** (41), 1–10.

Li, G., Gao, S., Zhang, G. & Zhang, X. 2014 Enhanced adsorption of phosphate from aqueous solution by nanostructured iron (III)-coper(II) binary oxides. *Chemical Engineering Journal* **235**, 124–131.

Liu, T., Wu, K. & Zeng, L. 2012 Removal of phosphorus by a composite metal oxide adsorbent derived from manganese ore tailings. *Journal of Hazardous Materials* **217–218**, 29–35.

Liu, Q., Hu, P., Wang, J., Zhang, L. & Huang, R. 2016 Phsophate adsorption from aqueous solutions by Zirconium(IV) loaded cross-linked chitosan particles. *Journal of the Taiwan Institute of Chemical Engineering* **59**, 311–319.

Lü, J. B., Liu, H. J., Liu, R. P., Zhao, X., Sun, L. P. & Qu, J. H. 2013 Adsorptive removal of phosphate by a nanostructured Fe–Al–Mn trimetal oxide adsorbent. *Powder Technology* **233**, 146–154.

Lu, J., Liu, H., Zhao, X., Jefferson, W., Cheng, F. & Qu, J. 2014 Phosphate removal from water using freshly formed Fe-Mn binary oxide: adsorption behaviors and mechanisms. *Colloid and Surface A: Physicochemical and Engineering Aspects* **455**, 11–18.

Maor, A. Z., Semiat, H. & Shemer, H. 2011 Adsorption-desorption mechanism of phosphate by immobilized nano-sized magnetite layer: interface and bulk interactions. *Journal of Colloid and Interface Science* **363**, 608–614.

Ogata, F., Imai, D., Toda, M., Otani, M. & Kawasaki, N. 2016 Properties of a novel adsorbent produced by calcination of nickel hydroxide and its capability for phosphate ion adsorption. *Journal of Industrial and Engineering Chemistry* **34**, 172–179.

Ogata, F., Ueta, E., Toda, M., Otani, M. & Kawasaki, N. 2017 Adsorption of phosphate ions from an aqueous solution by calcined nickel-cobalt binary hydroxide. *Water Science & Technology* **75**, 94–105.

Rodrigues, L. A. & da Silva, M. L. C. 2009 An investigation of phosphate adsorption from aqueous solution onto hydrous niobium oxide prepared by co-precipitation method. *Colloids and Surface A: Physicochemical and Engineering Aspects* **334**, 191–196.

Sposite, G. 1984 *The Surface Chemistry of Solids*. Oxford University Press, New York, NY, USA.

Wang, J., Liu, Y., Hu, P. & Huang, R. 2018 Adsorption of phosphate from aqueous solution by Zr(IV)-crosslinked quaternized chitosan/bentonite composite. *Environmental Progress & Sustainable Energy* **37**, 267–275.

Weng, C. H., Tsai, C. Z., Chu, S. H. & Sharma, Y. C. 2007 Adsorption characteristics of copper (II) onto spent activated clay. *Separation and Purification Technology* **54**, 187–197.

Yamashita, T., Ozawa, Y., Nakajima, N. & Murata, T. 1978 Ion exchange properties and uranium adsorption of hydrous titanium(IV) oxide. *Nippon Kagaku Kaishi* **8**, 1057–1061.

Yang, K., Yan, L. G., Yang, Y. M., Yu, S. J., Shan, R. R., Yu, H. Q., Zhu, B. C. & Du, B. 2014 Adsorptive removal of phosphate by Mg-Al and Zn-Al laered double hydroxides: kinetics, isotherms and mechanisms. *Separation and Purification Technology* **124**, 36–42.

Yu, Q., Zheng, Y., Wang, Y., Shen, L., Wang, H., Zheng, Y., He, N. & Li, Q. 2015 Highly selective adsorption of phosphate by pyromellitic acid intercalated ZnAl-LDHs: assembling hydrogen bond acceptor sites. *Chemical Engineering Journal* **260**, 809–817.

Zhang, G. S., Liu, H. J., Liu, R. P. & Qu, J. H. 2009 Removal of phosphate from water by a Fe–Mn binary oxide adsorbent. *Journal of Colloid and Interface Science* **335**, 168–174.

Zhang, C., Li, Y., Wang, F., Yu, Z., Wei, J., Yang, Z., Ma, C., Li, Z., Xu, Z. & Zeng, G. 2017 Performance of magnetic zirconium-iron oxide nanoparticle in the removal of phosphate from aqueous solution. *Applied Surface Science* **396**, 1783–1792.

First received 23 January 2018; accepted in revised form 6 June 2018. Available online 15 June 2018